International Journal of Automotive Technology, Vol. 24, No. 1, pp. 207–218 (2023)
DOI 10.1007/s12239–023–0019–4

pISSN 1229–9138/ eISSN 1976–3832

CHARACTERISTICS OF SPRAY NEAR THE NOZZLE AND TIP WETTING IN AN ENLARGED GDI INJECTOR STEP-HOLE NOZZLE

Byunggyun Kim[1)], Mengzhao Chang[2)] and Suhan Park[3)*]

[1)]Analysis & Evaluation Team, Hyundai Rotem, 37 Cheoldobangmulgwan-ro, Uiwang-si, Gyeonggi 16082, Korea
[2)]Department of Mechanics and Aerospace Engineering, Southern University of Science and Technology (SUSTech), Shenzhen 518055, China
[3)]School of Mechanical and Aerospace Engineering, Konkuk University, Seoul 05029, Korea

(Received 26 April 2022; Revised 18 July 2022; Accepted 19 August 2022)

ABSTRACT–This study is to analyze the spray characteristics near the nozzle according to the cavitating flow and step-hole structure using a quartz nozzle simulating a gasoline direct injection (GDI) injector. Referring to the dimensions of the injector used in mass-produced vehicles, various step-hole and injection pressure conditions were used in this experiment. Based on the injector dimensions, the step-hole conditions were designed in the direction of decreasing the depth and diameter. The internal flow in nozzle and spray near the nozzle were visualized by the shadow graphic and Mie-scattering visualization technique. A solenoid valve was used to simulate fuel injection like injector. Basically, the tendency of cavitating flow and spray characteristics were analyzed under various step-hole conditions. In addition, the tip wetting of nozzle with different step-hole conditions was analyzed, and the nozzle tip wettings at initial injection and end of the injection were separated and compared in detail. It was found that the wetting intensity decreased reduced 44.9 % when reduce step-hole depth from 2.5 to 1.5 mm. Tip wetting mainly occurred at initial injection for most step-hole conditions, but the tip wetting at end of injection was dominant when both decreasing the step-hole depth and step-hole diameter.

KEY WORDS : Cavitating flow, Nozzle step-hole, GDI injector, Characteristics of spray, Nozzle tip wetting

1. INTRODUCTION

Due to increasingly strict policies and regulations, particle number (PN) emissions from vehicles have become the focus of attention (Lee *et al*., 2020; Wang *et al*., 2014; Johnson, 2015; Song *et al*., 2018). In order to reduce to PN emission, Various attempts are underway, such as the optimization design of the injector structure (Moon *et al*., 2020; Chang *et al*., 2021; Chang *et al*., 2020), the development of new injection strategies (Sun *et al*., 2021) and combustion strategies (Jia *et al*., 2020; Jo *et al*., 2019), etc. Recently, it was found that the injector deposit is a main source of PN emissions (Fischer *et al*., 2018; Medina *et al*., 2020). There are 3 main reasons caused the PN emissions in direct injection (DI) engine due to injector deposit. First, injector deposits will lead to smaller spray cone angle and longer spray tip penetration, the possibility of spray impingement on the wall and the piston increases, which results in high PN emissions. Second, the atomization characteristics are deteriorated due to injector deposits, which leads uncompleted combustion and high soot formation. Third, for the deposit injector, an increasing of fuel leakage during injector closing and fuel storage in step-hole will lead to more diffusion flame, as a result, a higher PN emissions (Wen *et al*., 2016; Berndorfer *et al*., 2013). In addition to deteriorating the spray atomization characteristics and increasing PN emissions, deposit has also been found to reduce fuel economy (Zhang *et al*., 2020; Wang *et al*., 2017). Zhang *et al*. (2020) found that the indicated specific fuel consumption of deposit injector increased by 2 ~ 4.7 g/kWh compared to clean injector.

Injector deposits are mainly caused by the remining fuel in step hole and on nozzle tip. The non-evaporation high boiling point fuel will be remaining until next injection, which cause the uncompleted combustion and the formation of fuel deposits (Leach *et al*., 2018). It was found that higher injection pressure can play a role in cleaning the nozzle deposits. Through the combustion test, the deposit at injector tip under the injection pressure of 20 MPa is obviously less than that under the condition of 5 MPa (Kazour *et al*., 2014). In addition, injector tip deposits are expected to be reduced by decreasing the appearance of tip wetting. So, it is virtual important to study the formation mechanism of tip wetting and its influencing factors.

Tip wetting is usually studied by X-ray phase-contrast imaging technique and microscopic laser induced fluorescence (LIF) technique. However, visualization of fuel flow in transparent nozzle simulating a GDI injector

**Corresponding author*. e-mail: suhanpark@konkuk.ac.kr

provides another way to study tip wetting, which is low cost and easy to change in nozzle geometry.

Huang *et al.* (2019, 2021) studied the formation mechanism of tip wetting by using X-ray phase-contrast imaging technique. They found that under subcooled conditions, the needle bouncing at the end of injection has the most critical influence on the appearance of tip wetting, and the needle bouncing can be suppressed by increasing injection pressure. However, under flash boiling conditions, the tip wetting area increases during fuel injection. This is probably due to a large number of droplet breakup and enhanced plume-air interaction under flash boiling conditions, which is similar with the LIF visualization result by Leick *et al*. (2018). Yu *et al*. (2022) found that fuel with lower surface tension of leads to wider wetting area due to the stronger the spreading property of low surface tension. By computational fluid dynamics (CFD) simulation, Gavaises *et al*. (2021) found that the wall wetting of nozzle are more easy to occur during the closing and the re-opening period of the needle, due to the residual gases trapped insides the nozzle. Oh *et al*. (2017) visualized the side-view tip wetting of GDI injectors with different nozzle structures by using microscopic LIF technique, they found that the step hole surface area played a key role on the tip wetting area, the tip wetting area increases with the increasing of step hole surface. Leick *et al*. (2018) visualized the front-view tip wetting of GDI injectors, they found that the concentration distribution of tip wetting is reduced obviously by increasing injection pressure from 50 to 200 bar. Alzahrani *et al*. (2020) found that the tip drying time constant can be reduced by increasing the wetted area, the diffusion coefficient, the gas temperature, and the liquid vapor pressure of the wetted film.

According to the analysis above, tip wetting is effect by fuel temperature, injection pressure, nozzle geometry and so on. However, the effect of step hole on tip wetting is still unclear. The main novelty of this work is that the nozzle tip wetting of nozzles with different step hole sizes was studied by considering the injector internal flow and external flow in combination. In this study, the effect of the step hole structure and cavitation flow on the spray characteristics near the nozzle was investigated using a quartz nozzle simulating a GDI injector. In addition, in order to study to formation process of tip wetting, the nozzle tip wetting phenomenon according to the step hole geometry was analyzed by in injection initial stage and injection end stage.

2. EXPERIMENTAL APPARATUS

2.1. Experimental Setup

Figure 1 is a schematic view of the apparatus for visualizing spray and the cavitating flow in a step-hole nozzle. The working fluid can be pressurized within a range of up to 670 bar using a high pressure pump (Haskel, DSF-60) and a high pressure accumulator. A solenoid valve (SYNTEK, STH12C08) was used to simulate fuel injection like injector.

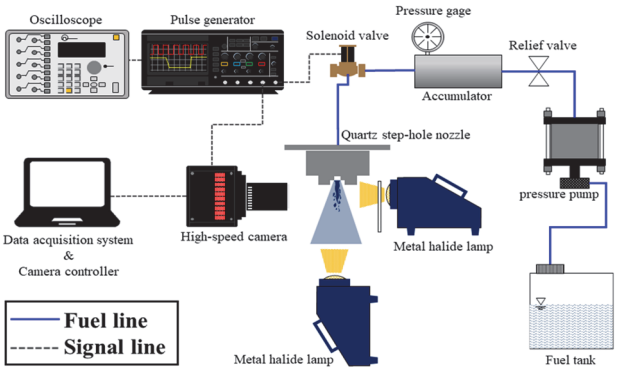

Figure 1. Schematic of experimental setup.

The injection pulse duration was controlled by a signal generator (Berkeley Nucleonics Corp., model 575) and an oscilloscope (TELEDYNE LECROY, WaveAce2014). Different from the use of the opening and closing of ball valves to control the injection of injectors, this study uses the solenoid valve to control the injection of nozzles. The advantage is to avoid the influence of the movement of the ball valve on the spray and tip wetting, and to more accurately reflect the influence of the nozzle structure on results. In addition, in order to acquire images during injection, the solenoid valve and the high-speed camera (FASTCAM, Mini AX100) were synchronized and controlled by a signal generator. The internal and external flows were visualized through the Mie-scattering and the shadow graph technique. High-speed camera and a metal-halide lamp (MID-25FC, 250 W) was used for image visualization. The ISO speed of the high-speed camera is 40,000 (black and white image) and 16,000 (color image), and the shutter speed ranges from 1.05 μs to 1 ms. Also, the maximum resolution is 1024×1024 pixels (4,000 FPS) and the minimum resolution is 128×16 pixels (540,000 FPS). Working fluid is n-heptane. There are 4 injection pressure conditions, 40 bar, 60 bar, 80 bar, and 100 bar, which were specified within the range of not damaging the quartz nozzle. The experiment was repeated 10 times to reduce the error between each condition. The focus of this paper is to study the effect of step hole structure on spray and tip wetting, so the experiments are carried out under the more easily achievable non-evaporative conditions of spray. Details of experiment conditions are shown in Table 1.

Figure 2 (a) shows parts of the injection device for injecting fuel, and it consists of a total of 4 parts. Fuel is supplied to the upper inlet called ‘upper cap’. After the quartz nozzle is mounted inside the ‘base’, the ‘nut’, the ‘washer’ and the ‘upper cap’ are combined. Since this is a high-pressure device in which fuel is injected at a maximum of 100 bar, silicon O-rings are used to maintain airtightness. Also, Figure 2 (b) shows the state in which all 4 parts are assembled.

Table 1. Experimental condition and fluid properties.

Injection pressure	40, 60, 80, 100 bar	
Injection pulse duration	20 ms	
Ambient pressure	Atmospheric (1 bar)	
Ambient temperature	Room condition	
Fuel (properties @295 K)	N-heptane (C_7H_{16})	
	Vapor pressure (Pa)	7000
	Density (kg/m^3)	684
	Dynamic viscosity (Ns/m^2)	0.000376
	Surface tension (mN/m)	19.65

(a) Part of injection equipment

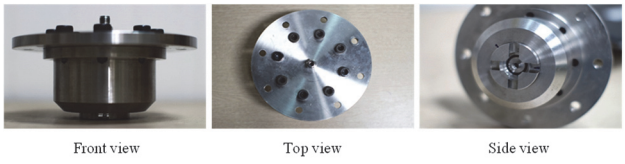

(b) Full assembly of injection equipment

Figure 2. Injection equipment.

Figure 3 is a schematic view of a quartz nozzle manufactured based on the dimensions of an injector. We referred to H Company's 250 bar kappa (κ) 1.0 T-GDI injector. The quartz nozzle used in this experiment was designed to be about 5 times scaled-up based on the injector, but the length-to-diameter ratio of hole were designed in the same as it. The hole length and diameter all nozzles were 1 mm and 1.5 mm, respectively. But the step-hole dimension

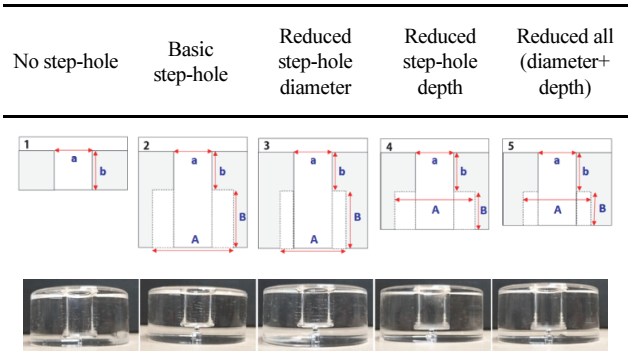

Nozzle type	Nozzle diameter (a)	Nozzle length (b)	Step-hole diameter (A)	Step-hole depth (B)
No step-hole	1 mm	1.5 mm	N/A	N/A
Basic step-hole	1 mm	1.5 mm	2.25 mm	2.5 mm
Reduced step-hole diameter	1 mm	1.5 mm	1.85 mm	2.5 mm
Reduced step-hole depth	1 mm	1.5 mm	2.25 mm	1.5 mm
Reduced all (diameter+depth)	1 mm	1.5 mm	1.85 mm	1.5 mm

Figure 3. Schematic of step-hole nozzle: shape of step-hole (reference injector: H Company, 250 bar κ 1.0 T-GDI).

has a total of five conditions: 'No step-hole condition', 'Basic step-hole condition, 'Reduced step-hole diameter', 'Reduced step-hole depth', and 'Reduced all'. More details refer to the Figure 3. The reason why the experimental conditions were set to decrease the diameter and depth of the step-hole is that the step-hole size of the recent injectors tends to be decreased in order to minimize the deposit due to wetting on the nozzle tip. So, a quartz step-hole nozzle was designed to observe and analyze internal flow and spray characteristics according to the tendency of reducing the step-hole size.

2.2. Visualization Methods

Figure 4 shows the visualization method used in this experiment. Shadow graph and Mie-scattering methods were used, and photographed in front view, side view, and bottom view for different purposes. The front view aims to observe the cavitating flow and spray characteristics, and the side view aims to observe the entire spray duration to analyze the nozzle tip wetting that occurs at the start and end of injection. Due to the limitations of the experimental apparatus, the camera is not parallel to the nozzle tip, so the result calculated from the side view is not the exact value of tip wetting, but the result can be used for quantitative comparison of tip wetting under different injection conditions. Lastly, the bottom view aims to observe the spray development near the nozzle at the beginning of injection.

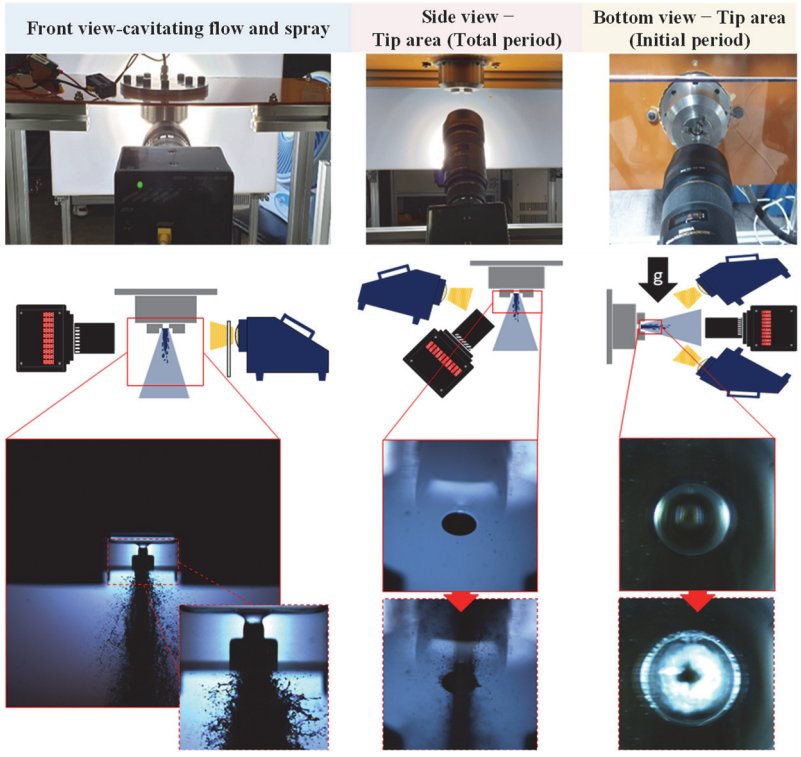

Figure 4. Method of image acquisition of cavitating flow and spray: shadow graph and Mie-scattering method.

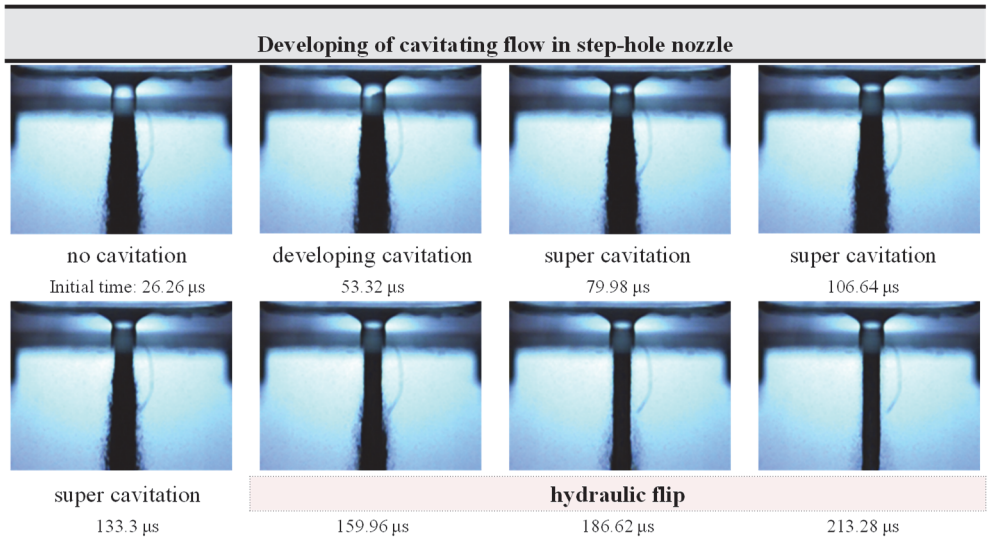

Figure 5. Development process of cavitating flow under different nozzle conditions.

3. RESULTS AND DISCUSSION

3.1. Cavitating Flow and Spray Atomization according to Injection Pressure

Figure 5 shows the process of cavitation and spray development, and this result showed similar trends to those obtained in our previous study (Kim and Park, 2019). The cavitating flow gradually grows as the pressure increases and is divided into the 4 steps: 'No cavitation', 'Developing cavitation', 'Super cavitation' and 'Hydraulic flip'. As the cavitation occurs, the spray angle gradually increases and the jet flow becomes violent. However, when it enters the

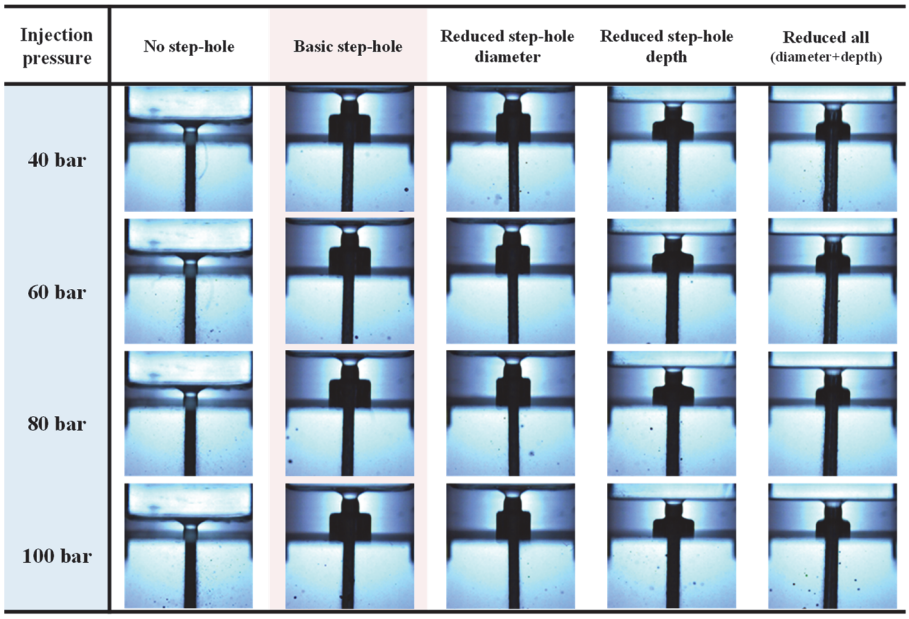

Figure 6. Cavitating flow according to nozzle conditions.

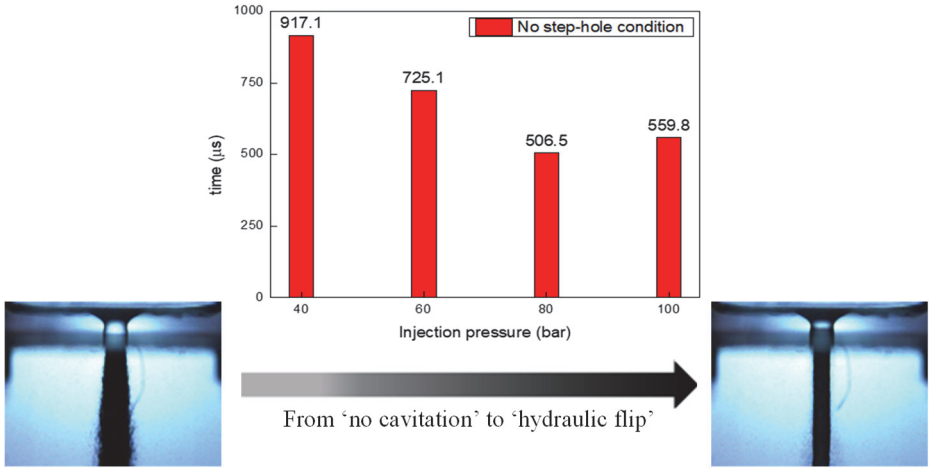

Figure 7. Total time from 'no cavitation' to 'hydraulic flip' according to injection pressure.

hydraulic flip, the spray angle decreases rapidly. In addition, the cavitating flow did not develop immediately into the hydraulic flip step as soon as injection started but developed through sequential steps like from 'No cavitation' to 'Hydraulic flip'. These results showed the same trend under all injection pressure conditions. Therefore, when fuel is injected from the injector, the flow inside the nozzle becomes very unstable because the cavitating flow undergoes a transient state. As a result, this situation will affect jet flow, atomization, and injector tip wetting at the beginning of injection. More detail about this will be explained in after section. The occur and development of cavitating flow are affected by external pressure, but since this study was conducted in the atmosphere, it was assumed that the conditions under which cavitating flow were the same for a nozzle without a step-hole and a nozzle with a step-hole.

Figure 6 shows the cavitating flow under all nozzle conditions. All images were taken after sufficient time for the cavitating flow to develop. Considering the above description, all nozzles correspond to the hydraulic flip step regardless of the injection pressure condition.

Figure 7 shows the total time required to develop from 'no cavitation' to 'hydraulic flip' depending on the injection pressure. As a result, cavitating flow develops more rapidly as the injection pressure increases. When the injection pressure increases, the fluid velocity increases, and when the

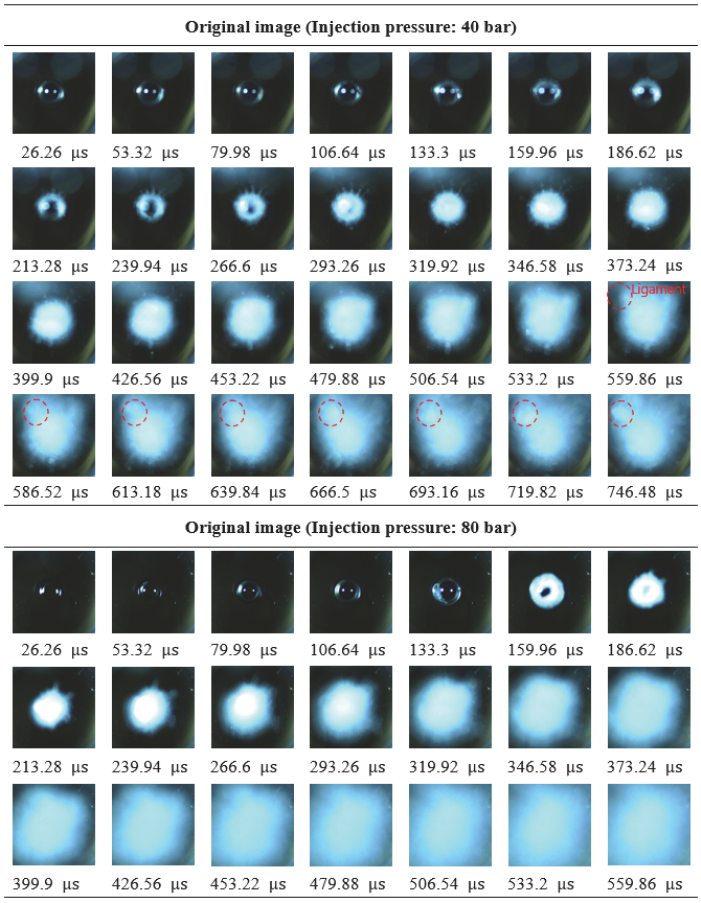

Figure 8. Development process of spray in the start of injection; injection pressure = 40, 80 bar. (a nozzle without a step-hole)

velocity increases, the Reynolds number increases. The Reynolds numbers for this study are approximately 196,468 at 40 bar and 311,074 at 100 bar. The detailed calculation procedure is presented in the discussion section (section 5). Therefore, it can be understood that the range of the Reynolds number belongs to the turbulent flow region in the flow in the pipe, and the turbulence intensity in the pipe gradually increases as the injection pressure increases.

Turbulence is known to affect the occurrence of cavitation. Vortex is the main component of turbulence, and nucleus in the flow can occur at the center of a vortex where the pressure level inside the nozzle is lower than the average or reference pressure. Assuming that the center of the vortex exists using the stream function of the vortex ($\psi = \frac{\Gamma}{2\pi} lnr,\ v_r = 0,\ v_\theta = -\frac{\Gamma}{2\pi r}$), the velocity at the center of the vortex increases infinitely. Also, according to Bernoulli's law, the pressure at the center of the vortex will decrease infinitely. Therefore, bubbles are generated when the central pressure of the vortex becomes lower than the saturated vapor pressure of the fluid. As a result, when the turbulence intensity increases over a certain level, it promotes the growth and development of cavitation (Shin *et al*., 2021; He *et al*., 2020). In addition, when the flow velocity increases as the injection pressure increases, the area (recirculation) in which the flow cannot flow along the shape of the nozzle inlet is expanded, and the nozzle inlet area where the static pressure decreases below the saturated vapor pressure is expanded. This means that the area where bubbles are generated increases. As a result, as the injection pressure increases due to such the complex things, the growth and development of cavitation is promoted, and the total time required for the cavitating flow to develop to the hydraulic flip is shortened. If the time required to develop from 'No cavitation' to the hydraulic flip is shortened, the time corresponding to each stage of cavitating flow will be shortened. In other words, the duration of super cavitation that affects nozzle tip wetting due to vigorous jet flow is reduced. This result is consistent with the tendency of the nozzle tip wetting to decrease at the initial injection as the injection pressure increases.

Figure 8 shows the process of spray development at the start of injection through cross section visualization under injection pressure condition of 40 bar and 80 bar. This series of images were acquired from a nozzle without a step-hole.

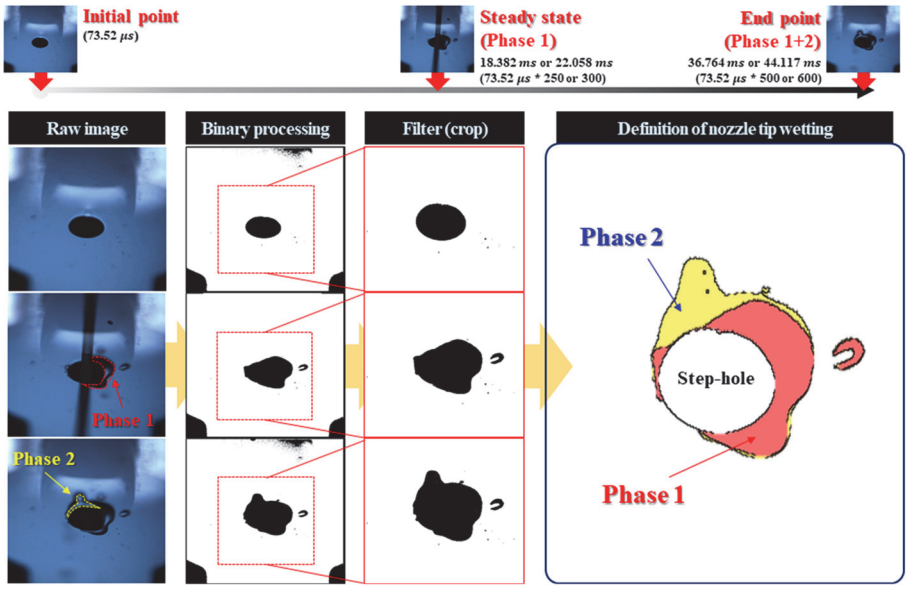

Figure 9. Definition and analysis method of nozzle tip wetting phenomenon.

There was a difference in spray development time and degree of atomization according to spray pressure conditions. At a injection pressure of 40 bar, ligament formed, which can be clearly seen on the outside of the spray. As the injection pressure increased to 80 bar, the atomization performance of the spray was significantly improved with the disappearance of the ligament, and the shape of the spray was more regular.

3.2. Characteristics of Nozzle Tip Wetting according to Step-hole Conditions

3.2.1. Definition of nozzle tip wetting

Figure 9 is the definition and analysis of the nozzle tip wetting phenomenon according to the step-hole condition. The nozzle tip wetting occurred in this study was defined in two stages depending on the cause of the occurrence. It is assumed that the nozzle tip wetting does not occur in the entire spray stage, but mostly occurs at a specific time point, such as the start and end of spray. Accordingly, the nozzle tip wetting was defined by subdividing into 'phase 1' and 'phase 2'. First, 'phase 1' is the nozzle tip wetting occurring in the initial stage of spray, and 'phase 2' is the nozzle tip wetting occurring in the end stage of spray. In order to quantitatively analyze the original image, binarization and filter processing were performed to investigate the proportion of each 'phase' in the whole nozzle tip wetting.

The injection process is divided into 'start of injection', the 'steady of injection', and the 'end of injection'. The 'start of injection' is the first image, the 'steady state' is when there is no change in spray behavior, and the 'end of spray' is when the spray is completely finished.

A filtered image was used to distinguish nozzle tip wetting that occurred in each 'phase'. For example, by subtracting the image of the start of injection from the image in the steady of injection, the nozzle tip wetting occupied in 'phase 1' can be grasped. And by subtracting the wetting of 'phase 1' from the wetting that occurred in the whole stage, the wetting that occurred at 'phase 2' can be found out.

3.2.2. Analysis of nozzle tip wetting according to step-hole conditions

Figure 10 shows the nozzle tip wetting according to the step-hole conditions based on the definition above. As can be seen from the image, there was a difference in tip wetting for each 'phase' according to the step-hole conditions. In this experiment, 'Reduced step-hole diameter' and 'basic step-hole', the tip wetting corresponding to 'phase 1' did not show any difference. Compared with this two step-hole conditions, the tip wetting corresponding to 'phase 1' of two step-hole conditions like 'Reduced step-hole depth' and 'reduced all' showed a tendency to decrease significantly. In addition, the tip wetting corresponding to 'phase 2' mainly occurs in the 'basic step-hole' condition and 'reduced all' condition. In particular, in the 'reduced all' condition, tip wetting of 'phase 2' shows opposite trend of 'phase 1' (tip wetting occurred very little in 'phase 1').

It was confirmed that most of the nozzle tip wetting occurred at the initial stage of spray and at the end stage of spray, but since the ratio of tip wetting occupied by each "phase" cannot be quantitatively checked according to the step-hole conditions, an additional definition was made.

$$Wetting\ \ intensity = \frac{Wetting\ \ area}{Step\ hole\ \ area} \quad (1)$$

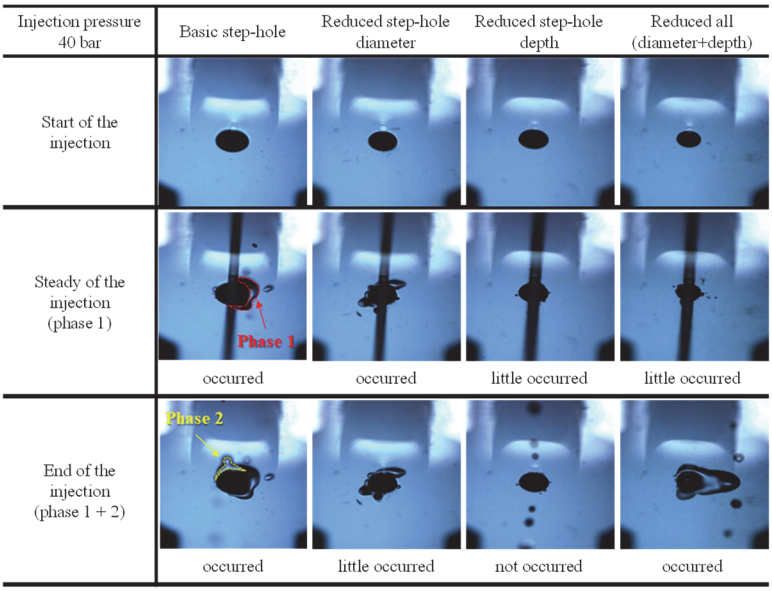

Figure 10. Images of nozzle tip wetting according to the step-hole conditions.

$$Wetting\ \ intensity\ of\ phase\ 1 = \frac{Wetting\ \ area\ of\ phase\ 1}{Wetting\ \ area} \quad (2)$$

$$Wetting\ \ intensity\ of\ phase\ 2 = \frac{Wetting\ \ area\ of\ phase\ 2}{Wetting\ \ area} \quad (3)$$

The dimensionless numbers indicated in (1) to (3) were calculated using the values obtained from the images to quantitatively analyze the nozzle tip wetting phenomenon. 'Wetting intensity' was defined by dividing the total wetting area by the step-hole area, which is used to evaluate the wetting level according to various nozzle conditions. This is because it was determined that the diameter of the step-hole was different according to each nozzle condition, and the influence on the wetting would be different accordingly. In addition, the wetting intensity of each phase represents the ratio of each "phase" area to the total nozzle tip wetted area. Based on the above definition of dimensionless numbers, we conducted investigation in more detail.

Figure 11 shows the wetting intensity in different phases according to the step-hole conditions in the four injection pressure conditions. Most of the tip wetting in the 'Reduced all' condition occurred in 'phase 2', which caused the largest wetting intensity of "reduced all" condition. However, in other step-hole conditions, most of the tip wetting occurs in 'phase 1'. That is, the degree of nozzle tip wetting is controlled according to the 'phase', and it was confirmed that the tip wetting according to the 'phase' can affect the total wetting intensity. Therefore, it is desirable to determine the tip wetting occurring in the injector by dividing the initial stage of spray and the end stage of spray, not the whole injection duration, and the injector tip wetting must be controlled by dividing each stage.

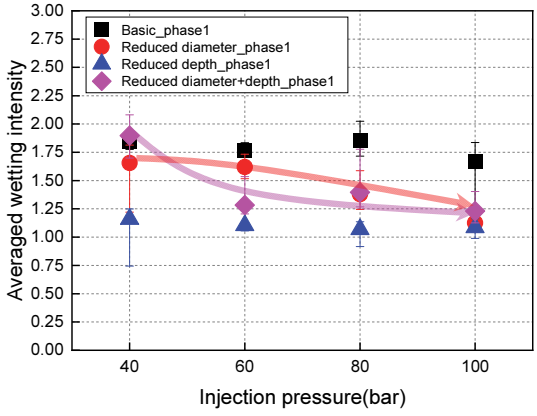

(a) Nozzle tip wetting fraction: phase 1

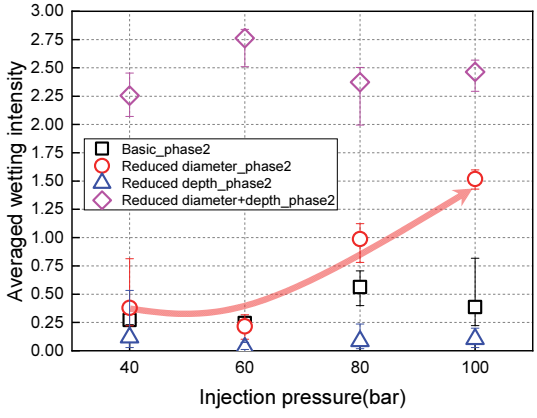

(b) Nozzle tip wetting fraction: phase 2

Figure 11. Nozzle tip wetting fraction according to the step-hole and injection pressure conditions.

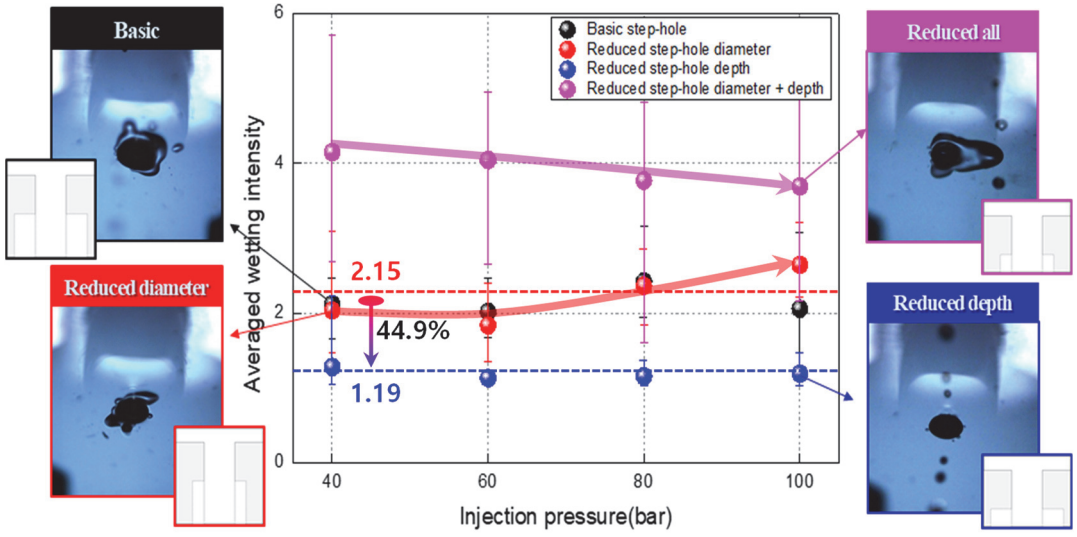

Figure 12. Nozzle tip wetting intensity according to the step-hole and injection pressure conditions.

According to the injection pressure, the wetting of each phase also showed a different tendency for different step-hole conditions. In Figure 11 (a), for 'Basic step-hole' and 'Reduced step-hole depth' condition, the wetting intensity in 'phase 1' remained relatively constant regardless of the injection pressure. However, in the 'Reduced step-hole diameter' and 'Reduced all' condition, the wetting intensity in 'phase 1' tended to decrease as the injection pressure increased. In Figure 11 (b), for 'Reduced step-hole diameter' condition, the wetting intensity in 'phase 2' tended to increase as the injection pressure increased.

At the end of the last injection, a large number of air bubbles formed in the nozzle due to air ingestion and fuel dripping (Moon *et al*., 2016). At the initial moment of injection, bubbles are broken by the increase of velocity, resulting in the formation of wetting in phase1 at the nozzle outlet. From Figure 11 (a), for the 'Reduced step-hole diameter' and 'Reduced all' condition, smaller diameters tend to allow the spray to adhere to the wall, producing a larger amount of wetting. As the injection pressure increases, the spray momentum increases. Due to the large momentum, spray ligaments or droplets can easily escape from the trapped wall even if they impinge on the wall. Therefore, under the 'Reduced step-hole diameter' and 'Reduced all' condition, the wetting decreases with the increase of the injection pressure.

On the other hand, at the end of injection, factors such as cavitation weakening and air ingestion cause the jet expansion inside nozzle. For the 'Reduced step-hole diameter' condition, the spray adhered easily to the wall of step hole. With the increase of the injection pressure, the width of the jet becomes wider, and more spray droplets adhere to the wall. After the spray droplets attached to the wall lose power, a large amount of wetting is formed at nozzle outlet. It can be concluded that nozzle structure size and injection pressure have a complicated influence on the wetting amount.

Figure 12 shows the wetting intensity according to the step-hole conditions under the 4 injection pressure conditions. Each is an average value of data obtained through 10 repeated experiments. 'Reduced all' condition showed the highest wetting intensity. 'Reduced step-hole diameter' and 'basic' condition showed similar middle wetting intensity. 'Reduced step-hole depth' condition showed the lowest wetting intensity. Compared to 'basic' condition, wetting intensity of 'Reduced step-hole depth' condition reduced 44.9 %.

In addition, it can be seen that the 'Reduced all' condition has a very large deviation compared to other conditions, which means the spray becomes very unstable at 'Reduced all' condition. As the wetting intensity decreases, the deviation also showed a decreasing trend. That is to say, when designing the injector, the increase or decrease of the step-hole dimension may reduce the injector tip wetting intensity, but the injector tip wetting intensity will be increased if the proper design is not accompanied. It can be concluded that only step-hole depth should be decreased to decrease PM emissions caused by tip wetting.

The effect of the injection pressure also showed a different tendency according to the step-hole conditions. It was shown that the wetting intensity was maintained relatively constant regardless of the injection pressure in the 'Basic step-hole' and 'Reduced step-hole depth' condition. However, under the 'Reduced all' condition, the wetting intensity tended to decrease as the injection pressure increased, and the opposite tendency was observed under the 'Reduced step-hole diameter' condition. The wetting intensity is determined by the wetting intensity of each phase.

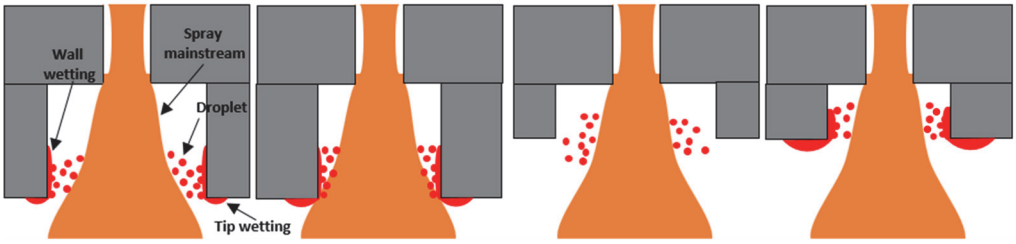

Figure 13. Schematic of step-hole wall wetting according to step-hole geometry.

Figure 13 is a schematic to explain the effect of step-hole dimension on tip wetting in detail. Since the hole length-to-diameter ratio are the same in this experimental condition, the spray angle will be relatively the same when injected from hole. According to the experiment results of Huang *et al*. (2019), small droplets of low velocity will be formed near the exit of the step-hole due to air entrainment. These small droplets hitting on the wall of the step-hole, thereby further forming tip wetting. When the diameter of the step-hole is reduced compared to the 'basic' condition, more droplets and spray hitting on the wall of the step-hole, resulting in more wetting. Conversely, when the step-hole depth is decreased, the possibility of droplets hitting on the step-hole wall is reduced, and as a result, less tip wetting occurs. However, when both decreasing the step-hole diameter and step-hole length, the possibility of droplets hitting on the step-hole wall increase, and droplets that tripped on the wall of step-hole are reduced due to reducing of step-hole surface, which caused more tip wetting.

It should be noted that the trend of stepped hole geometry will vary depending on the ratio of step hole diameter to hole diameter and hole L/D. This conclusion is mainly applicable to the case where the ratio of step hole diameter to hole diameter is 1.85 ~ 2.25 and hole L/D is about 1.5.

4. DISCUSSION

The purpose of this part is to discuss whether the conclusions of this work can be applied to GDI injectors. For the fluid inside the nozzle and outside the nozzle, Ca and Re are the two most important parameters that determine the flow state.

The calculation method of Ca is as follows:

$$Ca = \frac{P_a - P_v}{0.5\rho_l V^2} \tag{4}$$

where P_a is the ambient pressure, P_v is the saturated evaporation pressure, ρ_l is the fluid density, and V is the fluid velocity.

According to the Nuberly equation, the velocity of the nozzle outlet can be approximated by the following equation:

$$V \approx \sqrt{\frac{2P_l}{\rho_l}} \tag{5}$$

where P_l is the fluid pressure inside nozzle.

The Reynolds number is defined as follows:

$$Re = \frac{\rho_l V D}{\mu} \tag{6}$$

where D is diameter of nozzle, μ is viscosity of fluid.

In this experiment, the diameter of the nozzle is 1 mm, the injection pressure is 40 ~ 100 bar, and the parameter values of the fuel properties can be found in Table 1. Therefore, it can be calculated that the Ca of the transparent nozzle is $2.3\times10^{-2} \sim 9.3\times10^{-3}$, and Re is 196,468 ~ 311,074.

For GDI injectors, the nozzle diameter is usually 0.2 mm, and the injection pressure is usually 100 ~ 350 bar. Therefore, it can be calculated that the Ca of GDI injectors is $9.3\times10^{-3} \sim 2.7\times10^{-3}$, and the Re is 62,215 ~ 116,426.

Due to the limitation of the experimental conditions, the Ca and Re of the transparent nozzle and GDI injectors are not in the same range. But the Ca of both ($10^{-2} \sim 10^{-3}$) is much less than 1, that is to say, cavitation occurs inside the nozzle of both. In addition, the Re of both is greater than 2000, that is to say, the fluid flow of both is turbulent flow. Therefore, although the Ca and Re of the transparent nozzle and GDI injectors are not in the same range, it can be assumed that both will show the same trend, and the main conclusions of this study can be applied to GDI injectors.

5. CONCLUSION

In this study, the effect of injection pressure and step-hole conditions on spray and nozzle tip wetting characteristics was investigated. Under the same hole length-to-diameter ratio, the dimensions of the depth and diameter of the step-hole were changed to 4 cases, and the dimensions were referred to H company's 250 bar kappa (κ) 1.0 T-GDI

injector. The results of this study have important reference significance for optimizing injector performance in reducing tip wetting. The following conclusions were obtained.

(1) The cavitation flow developed with the same tendency regardless of the conditions. However, as the injection pressure increased, the cavitation flow developed faster and atomization was promoted more. In addition, the time point at which atomization is promoted is also faster.
(2) The nozzle tip wetting was defined as 'phase 1' and 'phase 2', which was based on the initial stage of spray and the end stage of spray. In addition, 'wetting intensity', which is dimensionless number, was defined to quantitatively analyze the phenomenon.
(3) Tip wetting occurred in 'phase 1' for most step-hole conditions. In the condition of 'Reduced all' and 'Reduced step-hole diameter', the wetting intensity of 'phase 1' tended to decrease as the injection pressure increased. It is thought that spray momentum increases as injection pressure increases. Spray droplets can easily escape from the trapped wall even if they impinge on the wall, which leads to less wetting with increasing injection pressure.
(4) In the condition of 'Reduced step-hole diameter', the wetting intensity of 'phase 2' tended to increase as the injection pressure increased, because of the wider jet width and lower spray velocity at end of injection.
(5) There was a difference in wetting intensity according to the step-hole condition. When the step-hole diameter was decreased, the trend was similar to the basic condition. When the step-hole depth was decreased, the wetting intensity decreased. However, when both the step-hole diameter and depth were decreased, the wetting intensity increased. In order to decrease PM emissions caused by tip wetting, only step-hole depth should be decreased.

ACKNOWLEDGEMENT–This study was financially supported under the Basic Science Research Program (2019R1A2C1089494) and the framework of the international cooperation program (2020 K1A3A1A19088692), funded by the National Research Foundation of Korea (NRF) under the India-Korea International Cooperation Program.

REFERENCES

Alzahrani, F. M., Fatouraie, M. and Sick, V. (2022). Analytical model for liquid film evaporation on fuel injector tip for the mitigation of injector tip wetting and the resulting particulate emissions in gasoline direct-injection engines. *Int. J. Engine Research* **23**, **1**, 49–63.

Berndorfer, A., Breuer, S., Piock, W. and Von Bacho, P. (2013). Diffusion combustion phenomena in GDI engines caused by injection process. *SAE Paper No*. 2013-01-0261.

Chang, M., Kim, H. I., Park, J. H., Wang, J. and Park, S. (2021). Ball motion and near-field spray characteristics of a gasoline direct injection injector using an x-ray phase-contrast imaging technique under high-injection pressures. *Int. J. Heat and Mass Transfer*, **166**, 120725.

Chang, M., Park, J., Kim, B., Park, J. H., Park, S. and Park, S. (2021). Effect of sac-volume on the relationship among ball behavior, injection and initial spray characteristics of ultra-high pressure GDI injector. *Fuel*, **285**, 119089.

EU Emission Standard: Cars And Light Trucks. https://dieselnet.com/standards/eu/ld.php

Fischer, A. and Thelliez, M. (2018). Methodology and tools to predict GDI injector tip wetting as predecessor of tip sooting. *SAE Paper No*. 2018-01-0286.

Gavaises, M., Murali-Girija, M., Rodriguez, C., Koukouvinis, P., Gold, M. and Pearson, R. (2022). Numerical simulation of fuel dribbling and nozzle wall wetting. *Int. J. Engine Research* **23**, **1**, 132–149.

He, Z., Zhou, H., Duan, L., Xu, M., Chen, Z. and Cao, T. (2021). Effects of nozzle geometries and needle lift on steadier string cavitation and larger spray angle in common rail diesel injector. *Int. J. Engine Research* **22**, **8**, 2673–2688.

Huang, W., Gong, H., Moon, S., Wang, J., Murayama, K., Taniguchi, H., Arima, T., Arioka, A. and Sasaki, Y. (2021). Nozzle tip wetting in GDI injector at flash-boiling conditions. *Int. J. Heat and Mass Transfer*, **169**, 120935.

Huang, W., Moon, S., Wang, J., Murayama, K., Arima, T., Sasaki, Y. and Arioka, A. (2020). Nozzle tip wetting in gasoline direct injection injector and its link with nozzle internal flow. *Int. J. Engine Research* **21**, **2**, 340–351.

Jia, H., Liu, Z., Yin, B., Xin, X. and Yi, X. (2020). Visualization research and optimization strategy for combustion process and emission characteristics of internal exhaust gas recirculation small non-road diesel engine. *Int. J. Automotive Technology* **21**, **2**, 481–492.

Jo, S., Park, S., Kim, H. J. and Lee, J. T. (2019). Combustion improvement and emission reduction through control of ethanol ratio and intake air temperature in reactivity controlled compression ignition combustion engine. *Applied Energy*, **250**, 1418–1431.

Johnson, T. V. (2015). Review of vehicular emissions trends. *SAE Int. J. Engines* **8**, **3**, 1152–1167.

Kazour, J., Befrui, B., Husted, H., Raney, M. and Varble, D. (2014). Innovative sprays and particulate reduction with GDi injectors. *SAE World Cong. & Exhibition*, Detroit, Michigan, USA.

Kim, B. and Park, S. (2019). Study on in-nozzle flow and spray behavior characteristics under various needle positions and length-to-width ratios of nozzle orifice using a transparent acrylic nozzle. *Int. J. Heat and Mass Transfer*, **143**, 118478.

Leach, F., Knorsch, T., Laidig, C. and Wiese, W. (2018). A review of the requirements for injection systems and the effects of fuel quality on particulate emissions from GDI engines. *SAE Paper No*. 2018-01-1710.

Lee, Z., Kim, T., Park, S. and Park, S. (2020). Review on

spray, combustion, and emission characteristics of recent developed direct-injection spark ignition (DISI) engine system with multi-hole type injector. *Fuel*, **259**, 116209.

Leick, P., Bork, B. and Geiler, J. N. (2018). Experimental characterization of tip wetting in gasoline DI injectors. *Proc. 14th Triennial Int. Conf. Liquid Atomization and Spray Systems (ICLASS)*, Chicago, Illinois, USA.

Medina, M., Alzahrani, F. M., Fatouraie, M., Wooldridge, M. S. and Sick, V. (2021). Mechanisms of fuel injector tip wetting and tip drying based on experimental measurements of engine-out particulate emissions from gasoline direct-injection engines. *Int. J. Engine Research* **22**, **6**, 2035–2053.

Moon, S., Huang, W., Li, Z. and Wang, J. (2016). End-of-injection fuel dribble of multi-hole diesel injector: comprehensive investigation of phenomenon and discussion on control strategy. *Applied Energy*, **179**, 7–16.

Moon, S., Huang, W. and Wang, J. (2020). Spray formation mechanism of diverging-tapered-hole GDI injector and its potentials for GDI engine applications. *Fuel*, **270**, 117519.

Oh, H., Lee, J., Han, S., Park, C., Bae, C., Lee, J., Seo, I. K. and Kim, S. J. (2017). Effect of injector nozzle hole geometry on particulate emissions in a downsized direct injection gasoline engine. *SAE Paper No*. 2017-24-0111.

Shin, S., Hong, J. W., Nagarathinam, D., Ahn, B. K. and Park, S. G. (2021). Tip vortex cavitation and induced noise characteristics of hydrofoils. *Applied Sciences* **11**, **13**, 5906.

Song, J., Lee, Z., Song, J. and Park, S. (2018). Effects of injection strategy and coolant temperature on hydrocarbon and particulate emissions from a gasoline direct injection engine with high pressure injection up to 50 MPa. *Energy*, **164**, 512–522.

Sun, Z., Cui, M., Ye, C., Yang, S., Li, X., Hung, D. and Xu, M. (2021). Split injection flash boiling spray for high efficiency and low emissions in a GDI engine under lean combustion condition. *Proc. Combustion Institute* **38**, **4**, 5769–5779.

Wang, B., Jiang, Y., Hutchins, P., Badawy, T., Xu, H., Zhang, X., Rack, A. and Tafforeau, P. (2017). Numerical analysis of deposit effect on nozzle flow and spray characteristics of GDI injectors. *Applied Energy*, **204**, 1215–1224.

Wang, C., Xu, H., Herreros, J. M., Wang, J. and Cracknell, R. (2014). Impact of fuel and injection system on particle emissions from a GDI engine. *Applied Energy*, **132**, 178–191.

Wen, Y., Wang, Y., Fu, C., Deng, W., Zhan, Z., Tang, Y., Li, X., Ding, H. and Shuai, S. (2016). The impact of injector deposits on spray and particulate emission of advanced gasoline direct injection vehicle. *SAE Paper No*. 2016-01-2284.

Yu, Y. S., Yang, S., Jeong, M., Kim, H., Yi, H., Park, J. H. and Park, S. (2022). Experimental investigations on the spray structure and nozzle tip wetting using various fuels with an LPDI injector. *Fuel*, **318**, 123719.

Zhang, W., Zhang, Z., Ma, X., Awad, O. I., Li, Y., Shuai, S. and Xu, H. (2020). Impact of injector tip deposits on gasoline direct injection engine combustion, fuel economy and emissions. *Applied Energy*, **262**, 114538.